Journal of Physics: Condensed Matter

PAPER • OPEN ACCESS

Direct observation of paramagnetic spin fluctuations in $LaFe_{13-x}Si_x$

To cite this article: Tom Faske *et al* 2020 *J. Phys.: Condens. Matter* **32** 115802

OPEN ACCESS
IOP Publishing
Journal of Physics: Condensed Matter
J. Phys.: Condens. Matter **32** (2020) 115802 (10pp)
https://doi.org/10.1088/1361-648X/ab5a99

Direct observation of paramagnetic spin fluctuations in $LaFe_{13-x}Si_x$

Tom Faske[1], Iliya A Radulov[1], Markus Hölzel[2], Oliver Gutfleisch[1] and Wolfgang Donner[1]

[1] Fachbereich Material- und Geowissenschaften, Technische Universität Darmstadt, Alarich-Weiss-Strasse 2, D-64287 Darmstadt, Germany
[2] Forschungsneutronenquelle Heinz Maier-Leibnitz (FRM II), Technische Universität München, Lichtenbergstrasse 1, D-85747 Garching, Germany

E-mail: wolfgang.donner@tu-darmstadt.de

Received 26 August 2019, revised 27 October 2019
Accepted for publication 22 November 2019
Published 16 December 2019

Abstract

Spin fluctuations are a crucial driving force for magnetic phase transitions, but their presence usually is indirectly deduced from macroscopic variables like volume, magnetization or electrical resistivity. Here we report on the direct observation of spin fluctuations in the paramagnetic regime of the magnetocaloric model system $LaFe_{11.6}Si_{1.4}$ in the form of neutron diffuse scattering. To confirm the magnetic origin of the diffuse scattering, we correlate the temperature dependence of the diffuse intensity with *ac* magnetic susceptibility and x-ray diffraction experiments under magnetic field. Strong spin fluctuations are already observable at 295 K and their presence alters the thermal contraction behavior of $LaFe_{11.6}Si_{1.4}$ down to the Curie temperature of the first-order magneto-structural transition at 190 K. We explain the influence of the spin fluctuation amplitude on the lattice parameter in the framework of the internal magnetic pressure model and find that the critical forced magnetostriction follows Takashi's spin fluctuation theory for itinerant electron systems.

Keywords: spin fluctuations, neutron scattering, phase transition, magnetocaloric effect, x-ray diffraction

S Supplementary material for this article is available online

(Some figures may appear in colour only in the online journal)

1. Introduction

The $LaFe_{13-x}Si_x$ system has been widely investigated in recent years because of the giant magnetocaloric effect (GME) that was observed for compositions $1.0 \leqslant x \leqslant 1.8$ [1, 2]. A potential application of materials exhibiting a GME is magnetic refrigeration—a technology that has the prospect of replacing conventional gas compressor refrigerator.s due to higher efficiency and environmental sustainability [3–6].

In our contribution, we present details on the mechanism of the phase transition in the $LaFe_{13-x}Si_x$ system by investigating the magnetostructural coupling and internal pressure related to spin fluctuations in $LaFe_{11.6}Si_{1.4}$.

$LaFe_{13-x}Si_x$ is a ferromagnetic material with a composition-dependent Curie temperature T_C. It is described as an itinerant-electron system in which the magnetic transition from the paramagnetic (PM) to a ferromagnetic (FM) state can be induced by either temperature or magnetic field, if applied just above T_C [1, 7, 8]. The magnetic transition is of first-order for compositions $x \leqslant 1.6$ [9] and, if induced by a magnetic field, is referred to as an itinerant-electron metamagnetic (IEM) transition [1, 8]. The change in internal energy during the IEM transition results in the GME and is dominated by changes in the electronic structure [10].

$LaFe_{11.6}Si_{1.4}$ exhibits a first-order PM–FM transition at $T_C \approx 190$ K that is accompanied by a giant spontaneous

magnetostriction of ~1.2% due to magnetovolume coupling [9, 11, 12]. It crystallizes in the cubic $NaZn_{13}$-type structure ($Fm\bar{3}c$ #226) in which the Fe atoms are located on two inequivalent Wyckoff sites (8*b* and 96*i*) with the La and Si atoms occupying the 8*a* and 96*i* sites, respectively [13]. The PM and FM phases are isostructural, apart from the difference in unit cell volume. The magnetically ordered phase has a simple FM spin structure and therefore no magnetic superlattice reflections appear in neutron diffraction patterns of the FM phase [12].

The paramagnetic state of $LaFe_{13-x}Si_x$ was recently described with a disordered local moment (DLM) model with a fluctuating Fe moment of ~1.9 μ_B [10, 14]. In accordance with this model, the temperature dependence of the reciprocal paramagnetic susceptibility χ^{-1} was found to obey the Curie–Weiss (CW) law for compositions $x > 1.6$ [9, 15–17]. Compositions of $LaFe_{13-x}Si_x$ with $x \leqslant 1.6$ also show CW behavior in the high-temperature regime, but in addition they exhibit a paramagnetic Curie temperature θ_p, as defined by the Bean–Rodbell model of magnetoelastic coupling [9, 18]. $\theta_p < T_C$ is characteristic for first-order transitions, and the larger $T_C - \theta_p$, the stronger the first-order character of the transition. Spin fluctuations terminate the FM state for first-order transitions before magnetic excitations realize the disappearance of collective magnetization and PM and FM phase therefore have different Curie temperatures [17]. For second-order transitions $\theta_p = T_C$ and no deviation from CW behavior is observed [9].

The two main contributions to spin fluctuations are thermally excited spin fluctuations and zero-point fluctuations. On cooling, one would expect the amplitude of thermal spin fluctuations ξ_{th} to decrease, whereas the amplitude of zero-point fluctuations ξ_{zp} increases, resulting in a net conservation of the squared sum $\xi_{th}^2 + \xi_{zp}^2 = \text{const}$ [19, 20].

Spin fluctuations as a driving force for magnetoelastic phase transitions have recently been discussed for other GME materials, such as rare earth manganites [21, 22], the $(Mn,Fe)_2(P,Si)$ system [23, 24] and Heusler compounds [25–27].

First-order phase transitions are generally described in terms of their Landau free energy. Spin fluctuations in itinerant-electron systems require a renormalization of the expansion coefficients in a Landau theory [7, 28] and had been introduced in the self-consistent renormalization (SCR) spin fluctuation theory by Moriya and Kawabata [20, 29]. The effect of spin fluctuations can be interpreted as an internal magnetic pressure that modifies the thermal expansion behavior [28, 30]. A deviation from linear thermal expansion can therefore be seen as evidence for the presence of strong spin fluctuations as Wada *et al* have demonstrated for $Y(Mn_{1-x}Al_x)_2$ and $Y_{1-x}Sc_xMn_2$ [31].

Takahashi proposed a theory describing the effect of spin fluctuations on the magnetic properties of itinerant-electron systems [20, 32]. According to Takahashi's theory, the magnetic pressure of spin fluctuations expresses itself in a fourth power of magnetization M^4 dependence of the forced magnetostriction $\Delta L/L$ at T_C as seen in the following equation:

$$\frac{\Delta L}{L} = \frac{\nu_h(M,\, T_C)}{\nu_0} = C \cdot \xi_{th}\,(0, T_C) \cdot \frac{M^4}{M_0^4(0)} \qquad (1)$$

where ν_0 and $\nu_h\,(M, T_C)$ represent the spontaneous and magnetic field-dependent volume contribution to magnetostriction, respectively. C is constant under isothermal conditions and $\xi_{th}(0,T_C)$ is the amplitude of thermal spin fluctuations in zero field. $M_0(0)$ represents the spontaneous magnetization and M the magnetization in a magnetic field.

The effect of spin fluctuations can not only be inferred indirectly in macroscopic variables like the volume or the magnetization: the direct proof for the occurrence of fluctuations is their detection by scattering methods.

Neutron scattering is a universal tool to investigate spin structures, both localized in a magnetically ordered system and disordered in the form of spin waves. The intensity of magnetically scattered neutrons in general is defined by the following equation (2): [33]

$$I_{mag}\,(Q) \sim \; |f_{mag}\,(Q)|^2 \sum_{\alpha,\beta} S^{\alpha,\beta}(Q,\omega)(\delta_{\alpha,\beta} - \hat{Q}_\alpha \hat{Q}_\beta) \qquad (2)$$

where $f_{mag}(Q)$ is the magnetic form factor, Q is the momentum transfer, ω is the energy transfer and the summation runs over the Cartesian directions. $S^{\alpha,\beta}(Q,\omega)$ is the magnetic scattering function which is proportional to the space and time Fourier transform of the spin-spin correlation function. The term $\delta_{\alpha,\beta} - \widehat{Q}_\alpha \widehat{Q}_\beta$ describes that neutron only probe the components of spin perpendicular to Q. If the energy of scattered neutrons is not analyzed, $I_{mag}(Q)$ is a snapshot of the spin correlations in reciprocal space.

In this contribution, we provide direct experimental evidence for the important role of itinerant spin fluctuations in the magnetic phase transition of $LaFe_{11.6}Si_{1.4}$. We report on evidence for paramagnetic spin fluctuations in $LaFe_{11.6}Si_{1.4}$ observed in the form of magnetic diffuse scattering in our temperature-dependent neutron powder diffraction data. Furthermore, we use x-ray diffraction to detect the effect of spin fluctuations on the lattice parameter, thereby verifying the 'internal pressure' effect of the fluctuations. Lastly, we confirm that the short-range magnetic correlations in $LaFe_{11.6}Si_{1.4}$ follow Takahashi's theory of spin fluctuations in itinerant-electron systems by using the example of the magnetization dependence of critical forced magnetostriction.

2. Experimental

2.1. Sample preparation

$LaFe_{11.6}Si_{1.4}$ was synthesized from elemental materials with commercial purity in a Al_2O_3 crucible using an induction furnace, as described in [34]. To prevent oxygen contamination, the elemental lanthanum was arc melted prior to induction melting with the other elements. To compensate for lanthanum losses due to evaporation, an excess of 7% La was added. For better homogeneity, the sample was re-melted twice in an induction oven under Ar pressure of 1 bar. Afterwards the

ingots were wrapped in Mo foil and sealed in fused silica tubes under 0.3 bar Ar pressure at RT. To form the desired 1:13 phase ($NaZn_{13}$-type structure), the ingots were annealed for 7 d at 1373 K in a resistive tube furnace and subsequently quenched in water.

2.2. Magnetic characterization

The magnetic moment measurements were performed using the vibrating sample magnetometer option of a QD PPMS 14 (Quantum Design Physical Property Measurement System, LOT-QuantumDesign GmbH). A needle shaped sample, cut from the bulk specimen, was used in order to minimize the demagnetization factor due to shape anisotropy. The PM–FM transition temperature T_C was determined from the temperature dependent magnetization measured in a magnetic field of 500 Oe from 300 to 100 K with a temperature sweep rate of 1 K min^{-1}.

The *ac* magnetic susceptibility was measured by means of an ACMS option of a QD PPMS 14 in an applied magnetic field of 10 kOe. The temperature dependent measurement was performed on cooling from 350 to 100 K in an alternating excitation field with frequency of 1 kHz and amplitude of 10 Oe.

2.3. Neutron diffraction

Unpolarized neutron diffraction experiments were performed at the high-resolution diffractometer SPODI at research reactor FRM II, Garching [35]. The wavelength was set to $\lambda = 1.5482$ Å by a stack of Ge(5 5 1) monochromator crystals. A cylinder (11 × 18 mm, ~11 g) cut from polycrystalline bulk $LaFe_{11.6}Si_{1.4}$ was placed in a cylindrical vanadium container and into a closed-cycle helium cryostat. Diffraction patterns were collected on cooling in the temperature range from 295 to 5 K between 3.2 and 160° in 2θ ($Q = 8.0$ Å^{-1}) with a step size of 0.05°. Rietveld analyses of the neutron diffraction patterns were performed up to $2\theta = 135°$ ($Q = 7.5$ Å^{-1}) using the FullProf program, which allows for the simultaneous refinement of structural and magnetic profiles [36, 37]. The diffraction range $Q > 7.5$ Å^{-1} was excluded from Rietveld analysis due to instrument-related broadening of the reflections, which could not be modelled using the same peak shape function as for the rest of the pattern.

2.4. X-ray diffraction

Temperature and magnetic field-dependent x-ray diffraction patterns were collected on a custom-built diffractometer in transmission geometry (Mo K_α radiation, $\lambda_1 = 0.70932$ Å, $\lambda_2 = 0.71332$ Å, MYTHEN2 R 1K detector (Dectris Ltd), 2θ range from 7 to 67°, step size of 0.009°). A detailed description of the diffractometer can be found in [38]. A piece of bulk $LaFe_{11.6}Si_{1.4}$ from the neutron diffraction experiments was crushed and mixed with a NIST640d standard reference silicon powder for correction of geometric errors. The temperature was controlled by means of a closed-cycle helium cryofurnace (SHI Cryogenics Group) in the range from 400 to 12 K. The cooling rate was 2 K min^{-1} and the sample temperature was stabilized for 10 min before data collection. Measurements were performed for zero-field cooling (ZFC) and field-cooled cooling (FCC) protocol under 1.0, 3.0 and 5.0 T applied magnetic field. Structural parameters were again refined using the Rietveld option of the FullProf software.

3. Results and discussion

3.1. Neutron diffraction

In order to probe the magnetostructural coupling in $LaFe_{11.6}Si_{1.4}$, we performed temperature-dependent neutron diffraction experiments. Diffraction patterns of bulk $LaFe_{11.6}Si_{1.4}$ were collected on cooling between 295 K and 5 K. Typical neutron diffraction patterns and corresponding Rietveld analyses are shown in figure 1(a) for $T = 295$ K and figure 1(b) for $T = 5$ K. Phase purity is confirmed aside from ~1 wt.% fraction of α-Fe side phase. The small goodness-of-fit (χ^2) and residual (R) values from Rietveld refinement of profile (R_f), peak positions (R_{Bragg}) and (below T_C) magnetic structure (R_{mag}) suggest an excellent data quality and a well-fitting structure model. The temperature of the onset of magnetic transition $T_{tr} = 200$ K is identified by a splitting of all Bragg reflections, see figure 1(c). PM and FM phase coexist in the temperature range from 200 to 191 K and the magnetic transition is complete at the Curie temperature $T_C = 190$ K.

First traces of the FM phase appear in the neutron diffraction pattern at T_{tr}, identified by a splitting and shift of all reflections to lower Q due to giant spontaneous magnetostriction, see figure 1(c). The observed coexistence of PM and FM phase is characteristic for a nucleation and growth process of first-order phase transitions, as it is expected for $LaFe_{11.6}Si_{1.4}$ [9, 12]. The lattice parameter of the FM phase a(FM) is significantly larger than that of the PM phase a(PM), see figure 2 and it further expands on cooling in the two-phase region, due to the increasing spontaneous Fe magnetic moment [12].

Apart from ~1% volume expansion, the crystal structure of the PM phase of $LaFe_{11.6}Si_{1.4}$ is retained in the FM phase. Figure 3(a) shows a contour plot of the temperature dependence of the low Q region from 295 to 5 K. The neutron diffraction patterns of the PM and FM phases display the same number of reflections, however, several Bragg reflections such as 2 0 0 and 2 2 0 gain intensity during the magnetic transition.

Strong diffuse intensity I_{diff} is present above T_C in the low Q range up to $Q \approx 0.8$ Å^{-1}, see figure 3(b). On cooling from 295 K, I_{diff} first increases and peaks at $T = 200\,\text{K} = T_{tr}$ but sharply drops thereafter. Simultaneously to the decrease in I_{diff}, the 2 0 0 and 2 2 0 Bragg reflections gain intensity due to FM contributions. The integrated intensity of Bragg reflections $I_{Bragg}(hkl)$ in neutron diffraction consists of two contributions: $I_{Bragg}(hkl) = I_{nuc}(hkl) + I_{mag}(hkl)$, where $I_{nuc}(hkl)$ is the nuclear and $I_{mag}(hkl)$ the magnetic contribution due to long-range spin ordering. The close relation between I_{diff} and $I_{mag}(hkl)$ is a hint towards a magnetic origin of I_{diff}, such as short-range FM correlations. Neutron diffraction studies published previously on the $LaFe_{13-x}Si_x$ system, however, do not

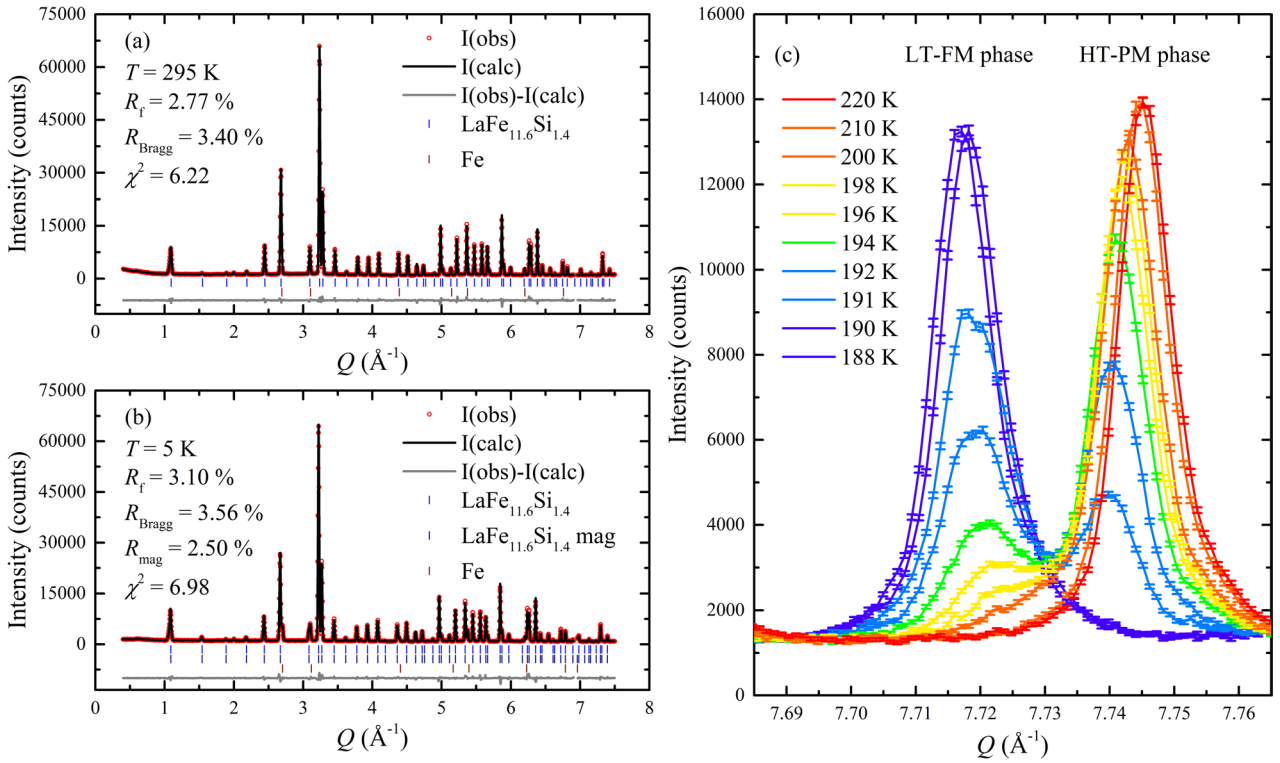

Figure 1. Rietveld refinement of the neutron diffraction pattern of $LaFe_{11.6}Si_{1.4}$ collected at (a) $T = 295$ K and (b) $T = 5$ K. Observed (red dots), calculated (black line) and difference (grey line) patterns are given, as well as reflection positions for $LaFe_{11.6}Si_{1.4}$ (blue), magnetic $LaFe_{11.6}Si_{1.4}$ (dark blue) and a side phase of ~1 wt.% α-Fe (wine). Structural parameters from the Rietveld refinement are listed in supplementary table S1 (available online at stacks.iop.org/JPhysCM/32/115802/mmedia). (c) Splitting and shift of high Q nuclear reflection 10 8 6 of $LaFe_{11.6}Si_{1.4}$ on cooling over the magnetic ordering temperature. The high-temperature paramagnetic HT-PM and low-temperature ferromagnetic LT-FM phase coexist in the temperature range from 200 to 191 K.

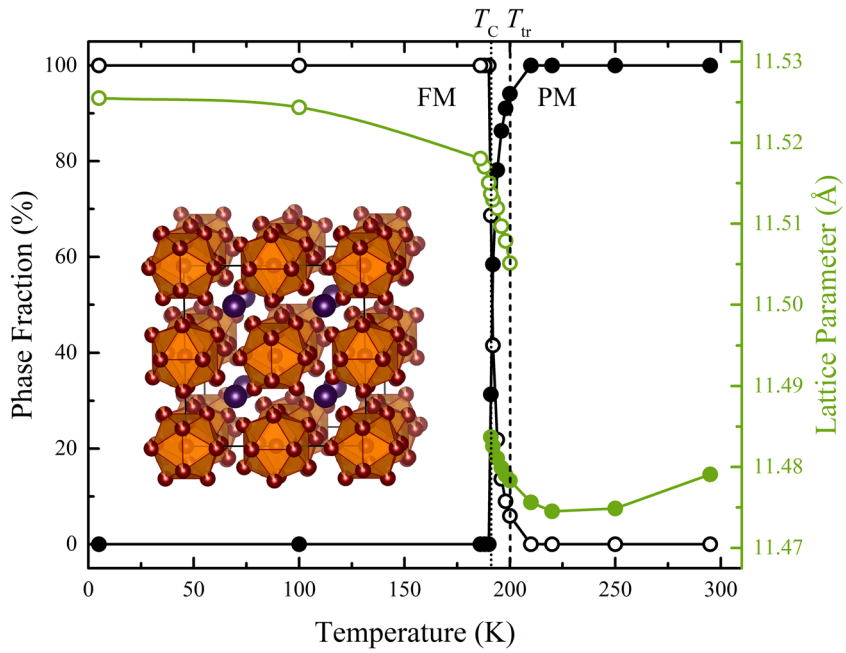

Figure 2. Phase fraction (left) and lattice parameter (right) of the paramagnetic PM (filled circles) and ferromagnetic FM phase (open circles) obtained from Rietveld refinements of neutron diffraction data of bulk $LaFe_{11.6}Si_{1.4}$. The dashed line marks the onset of magnetic transition at temperature $T_{tr} = 200$ K. The dotted line shows the Curie temperature $T_C = 190$ K. Symbols are connected by spline curves serving as guides to the eye. The inset shows the crystal structure of $LaFe_{11.6}Si_{1.4}$ with two distinct Fe atoms (wine), Si (orange) partially occupying the Fe position on polyhedral corners and La (purple) occupying large voids in between Fe/Si polyhedra [39].

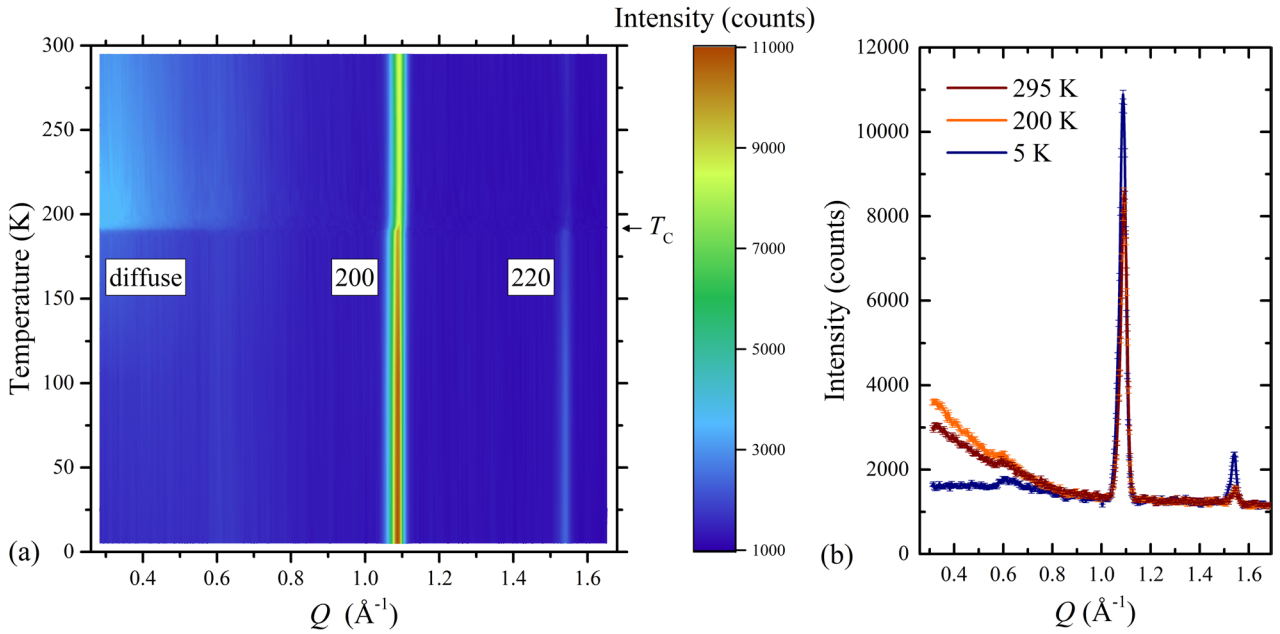

Figure 3. (a) Contour plot of neutron diffraction data measured for bulk $LaFe_{11.6}Si_{1.4}$ on cooling in the temperature range 295 to 5 K. Small angle diffuse scattering (top-left) and Bragg reflections 200 and 220 are marked. (b) Raw neutron diffraction patterns collected at 295, 200 and 5 K.

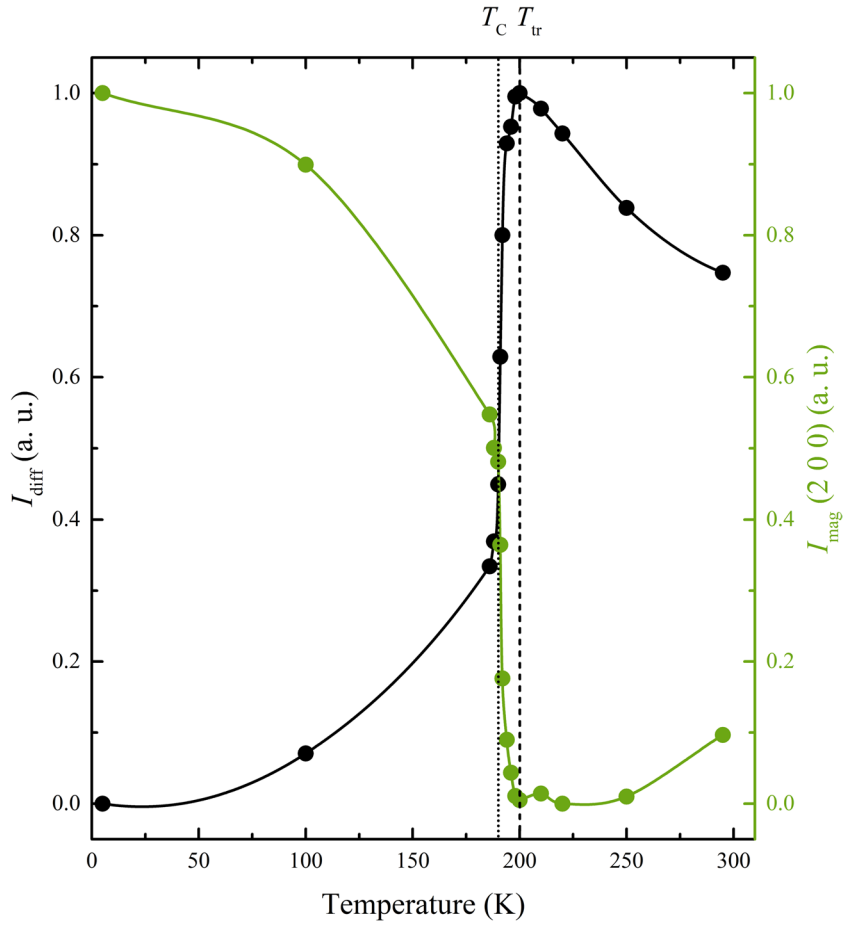

Figure 4. Evaluation of the temperature dependence of magnetic scattering intensity from neutron diffraction data of bulk $LaFe_{11.6}Si_{1.4}$. Integrated magnetic diffuse scattering I_{diff} (left) and normalized 200 magnetic Bragg reflection intensity $I_{mag}(200)$ (right) are shown. The dashed line marks the onset of magnetic transition at temperature $T_{tr} = 200$ K. The dotted line shows the Curie temperature $T_C = 190$ K. Symbols are connected by spline curves serving as guides to the eye.

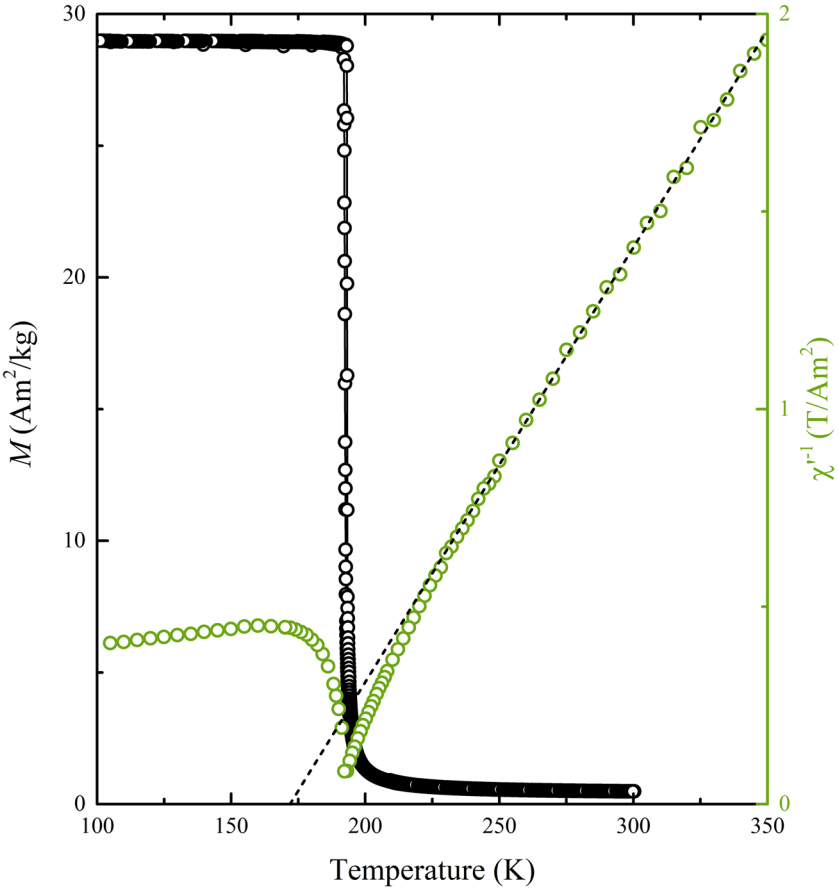

Figure 5. Temperature dependence of the magnetization M (left) of bulk $LaFe_{11.6}Si_{1.4}$ under an applied field $\mu_0 H = 0.05$ T and the inverse of the real part of the *ac* susceptibility χ'^{-1} (right) measured at 1 T. The dashed line shows a linear fit of χ^{-1} in the paramagnetic regime according to Curie–Weiss law.

show the low Q region and thus do not allow for comparison with our work [12, 13, 40].

We integrate the area under the curve like $I_{\mathrm{diff}} = \int_{0.3\,\text{Å}^{-1}}^{0.8\,\text{Å}^{-1}} I\,(Q)\,\mathrm{d}Q$ in order to quantify the diffuse scattering contribution, see figure 4. Sizable I_{diff} is already present at 295 K (1.55 T_{C}). Upon cooling, I_{diff} increases approaching T_{C} and has a maximum at $T_{\mathrm{tr}} = 200$ K (1.05 T_{C}). I_{diff} sharply drops with the appearance of FM phase in the temperature range between T_{tr} and T_{C} and is converted into $I_{\mathrm{mag}}(h\,k\,l)$. At $T = 186$ K (0.98 T_{C}), however, despite the magnetic transition being complete, I_{diff} is still ~33 % of the value at T_{tr}, as can be seen in figure 4. A further conversion of the remaining I_{diff} to $I_{\mathrm{mag}}(h\,k\,l)$ continues down to 5 K. An explanation for significant I_{diff} being present below T_{C} is that the magnetization is not yet saturated. Consequentially, the conversion of remaining I_{diff} to $I_{\mathrm{mag}}(h\,k\,l)$ continues in the FM phase down to 5 K. The further increase in I_{diff} far below T_{C} indicates that the localized Fe magnetic moment increases up to its saturation value of 2.16 μ_{B} at 0 K [12].

3.2. Magnetization and ac magnetic susceptibility

As shown in figure 5, the $LaFe_{11.6}Si_{1.4}$ compound shows a sharp PM–FM transition in the *dc* magnetization measurements with a small thermal hysteresis of ~1 K. We can conclude from the sharp transition that the sample is chemically homogeneous. The small remnant magnetization above T_{C} proves that only low amounts of FM impurities such as α-Fe are present. $T_{\mathrm{C}} = 191$ K is in perfect agreement with T_{C} obtained from neutron diffraction.

The spontaneous magnetization amounts to 22.62 μ_{B}/f.u. at 5 K; consequently one can extract an average value for the mean Fe magnetic moment. The average moment per Fe atom (μ_{Fe}) is estimated to be 1.95 μ_{B}/Fe. Magnetic measurements have been recorded at high temperatures, well above the magnetic transition temperature, in order to investigate the magnetic behavior of Fe in the paramagnetic state. At high temperatures, the thermal variation of the reciprocal magnetic susceptibility shows a CW behavior. A linear fit of the experimental data according to a CW law leads to a Curie constant $C = 67.9$ μ_{B}K/f.u.T. The effective paramagnetic moment μ_{eff} deduced from the Curie constant is found to be 5.10 μ_{B}/Fe. The investigation of the magnetic properties in both paramagnetic and ferromagnetic states has led to significantly different values of Fe magnetic moments in magnetically ordered state ($\mu_{\mathrm{Fe}} = 1.95$ μ_{B}/Fe) and in the disordered state ($\mu_{\mathrm{eff}} = 5.10$ μ_{B}/Fe). This leads to a number of spin $S_{\mathrm{p}} = 2.10$ and $S_0 = 0.975$ in the paramagnetic and the ferromagnetic state respectively and a corresponding Rhodes–Wohlfarth ratio $r = S_{\mathrm{p}}/S_0$ of 2.15. This points to the itinerant character of magnetism in the present compound.

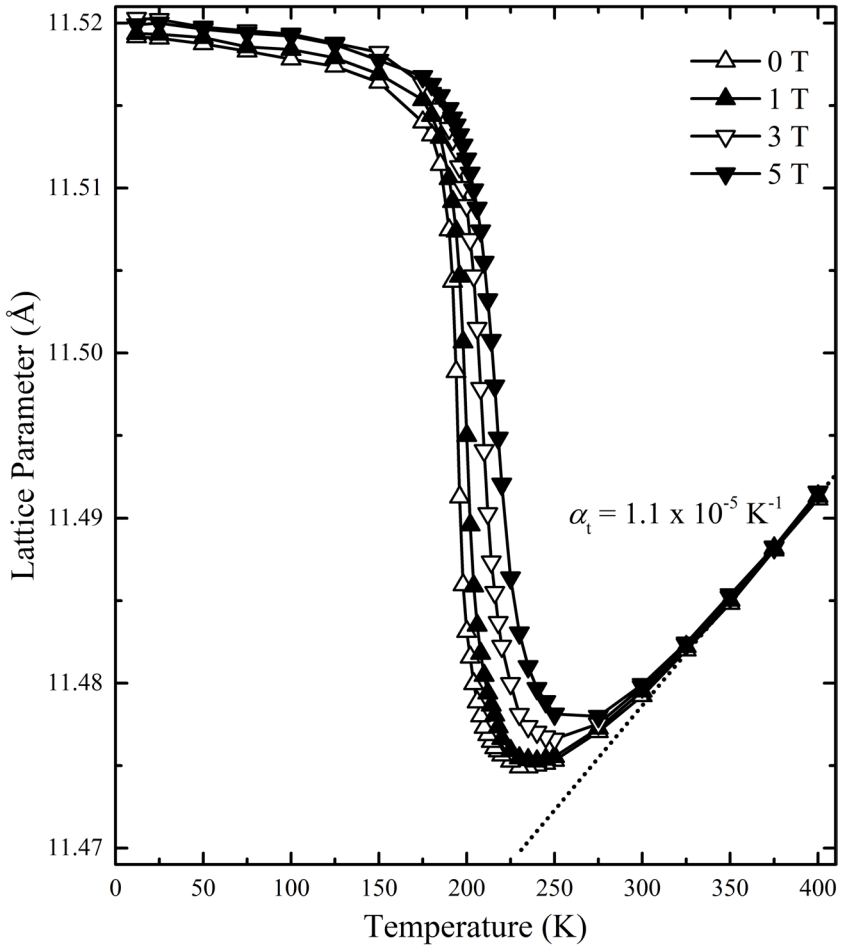

Figure 6. Lattice parameter of $LaFe_{11.6}Si_{1.4}$ powder determined by x-ray diffraction for ZFC and FCC protocol in magnetic fields of 1, 3 and 5 T. The dotted line shows the extrapolation of linear thermal contraction above T_C.

Since the obtained value of r is larger than 1, we expect that the amplitude of local spin fluctuations varies significantly with temperature in this system, according to the SCR theory of spin fluctuations [41–43]. In this model, two extreme regimes characterized by different values of the Rhodes–Wohlfarth ratio r, are described: (i) local moment limit and (ii) weakly ferromagnetic limit. In the local moment limit we have $r = 1$ and in the opposite weakly ferromagnetic limit the theoretical model predicts a divergence of this ratio.

The inverse of the real part of the *ac* susceptibility χ'^{-1} shows CW behavior in the PM regime as predicted for itinerant ferromagnets by Moriya and Kawabata [29] and for the $LaFe_{13-x}Si_x$ system in particular by Fujita [14], but deviates from linearity at $T_{CW} = 225$ K. This change of slope in χ^{-1} close to T_C is expected for first-order transitions according to the Bean–Rodbell model [18]. We extracted a paramagnetic Curie temperature $\theta_p = 170$ K that is close to the value reported for $LaFe_{11.8}Si_{1.2}$ [9]. The large difference $T_C - \theta_p$ confirms the strong first-order nature of the phase transition.

3.3. Magnetic field and temperature-dependent x-ray diffraction

Figure 6 shows the thermal evolution of the lattice parameter of $LaFe_{11.6}Si_{1.4}$ determined from x-ray powder diffraction on cooling for different magnetic fields. Extracting separate lattice parameters a(PM) and a(FM) in the transition region was not possible because of the lower angular resolution of our x-ray compared to our neutron diffraction experiments. The PM–FM transition of $LaFe_{11.6}Si_{1.4}$ powder is not as sharp as for bulk material, which is a known effect for a powder due to decoupling of the particles [44]. We found the thermal expansion to be linear for $T > 300$ K with an expansion coefficient $\alpha_t = 1.1 \times 10^{-5}$ K^{-1}, independent of magnetic field. Jia *et al* reported a value of $\alpha_t = 8.2 \times 10^{-6}$ K^{-1} [9] for the temperature range 300–250 K. Our data show, however, that the thermal expansion is not linear in the temperature range used for determination of the reported α_t. Deviation from linear behavior starts at $T \approx 300$ K, most likely due to the appearance of short-range magnetic correlations. Overcompensation of thermal contraction under zero applied field starts at the temperature $T_{comp} = 225$ K, resulting in a net increase in a(PM) upon further cooling and a sharp expansion at $T_C = 194$ K.

Applying a magnetic field during cooling shifts T_C towards higher temperatures at a rate of ~4 K T^{-1}, which is consistent with previous studies [1, 9]. The magnetic transition is broader for larger magnetic fields due to an increasing second-order character of the IEM [1]. Simultaneously with T_C, T_{comp} also increases with increasing magnetic field, whereas the high-temperature behavior above $T > 300$ K is identical for all

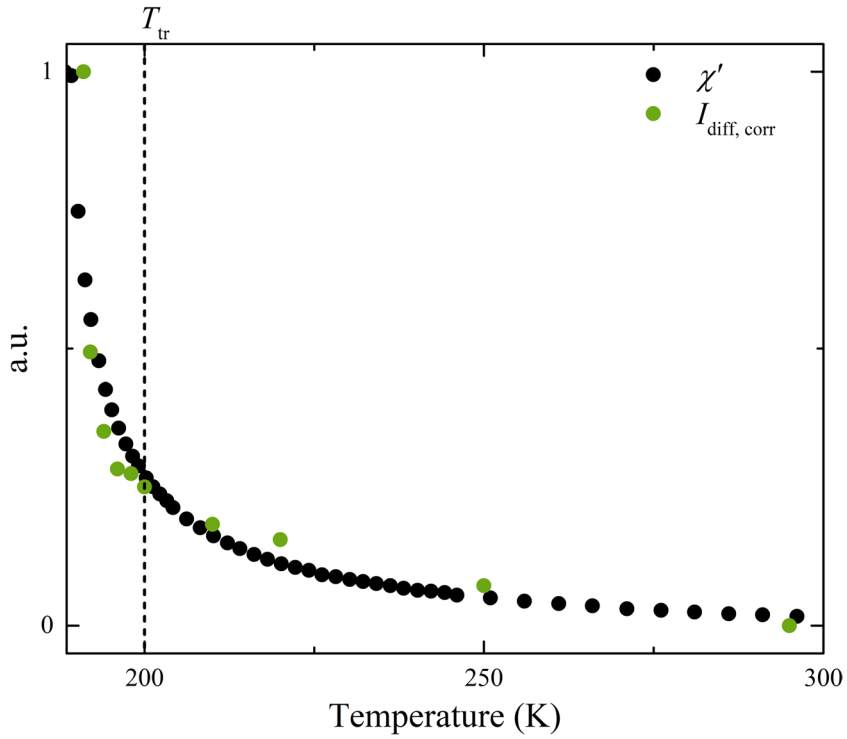

Figure 7. Comparison of the real part of the *ac* magnetic susceptibility χ' under $\mu_0 H = 1$ T (black) and $I_{diff,corr}$ (green) normalized to 1. The dashed line highlights the temperature of onset of magnetic transition $T_{tr} = 200$ K.

magnetic fields. We assume that the magnetic field enhances the short-range magnetic correlations in the PM regime at $T < 300$ K of $LaFe_{11.6}Si_{1.4}$. Therefore, T_{comp} increases with increasing field—eventually inducing the IEM transition at $T > T_C(0\ T)$. Below T_C we observe a small increase in a(FM) with increasing magnetic field due to forced magnetostriction and saturation of magnetization far above 0 K.

4. Discussion

4.1. Diffuse Scattering

We integrate the diffuse signal shown in figure 3(b) up to $Q = 0.8$ Å^{-1}, which is justified by the fact that the maximum momentum transfer of spin fluctuations in Fe is $Q_{max} \approx 0.75$ Å^{-1} [45] Spin fluctuations transition into the Stoner continuum at larger Q values and our I_{diff}, therefore, covers all essential magnetic fluctuations. We consider the fluctuation-dissipation theorem [46] to show that I_{diff} in our neutron diffraction data is indeed a good proxy for ξ. However, the maximum of the as-observed I_{diff} at T_{tr} does not necessarily translate to a maximum of ξ. The reason being that the PM–FM transformation begins at T_{tr} and spans over a 10 K temperature window. I_{diff} decreases proportionally to the PM fraction (W_{PM}) between T_{tr} and T_C whereas $I_{mag}(hkl)$ increases proportionally to the FM fraction (W_{FM}). If we assume that I_{diff} originates only from the PM phase, we can correct I_{diff} above T_C by dividing through W_{PM}.

Figure 7 shows the comparison of $I_{diff,corr} = I_{diff}/W_{PM}$ with the real part of the *ac* susceptibility χ'; the fact that they both show the same temperature dependence is evidence that $I_{diff,corr}$ measures ξ. We can now use $I_{diff,corr}$ instead of equation (2), while the error that we make by final integration in space and time is small, since $f_{mag}(Q)$ is a function that decays fast. ξ, consequentially, increases continuously down to T_C.

4.2. Lattice parameter—internal magnetic pressure

We observe linear thermal contraction for $LaFe_{11.6}Si_{1.4}$ at temperatures above $T > 300$ K. Deviation from linear behavior starts below $T \approx 300$ K and is present in both, our neutron and x-ray diffraction data, see figures 2 and 6, respectively. Simultaneously, our neutron diffraction data reveals that strong magnetic fluctuations are present in the form of I_{diff} at $T = 295$ K, see figure 3. I_{diff}, as shown in section 4.1, is a measure for ξ and increases on cooling, until it diverges at T_C. At the same time, the lattice parameter deviates further from high-temperature linear behavior the closer the temperature gets to T_C. Below $T_{comp} = 225$ K, the lattice parameter even increases upon further cooling. A feature that is likely related is present in our *ac* susceptibility data, where we observe a deviation from CW behavior at the same temperature $T_{CW} = 225$ K, see figure 5.

In the two-phase region we observe a sharp increase in lattice parameter not only for the FM phase, but also for the PM phase. a(FM) is expected to increase due to spontaneous magnetostriction as the Fe magnetic moments assume long-range order [12]. The trend of a(PM), however, cannot be explained by magnetostriction. Instead, we use the model of internal magnetic pressure by Wagner and Wohlfarth. According to their theory, spin fluctuations exert a magnetic pressure proportional to ξ and thus influence a system's lattice parameter

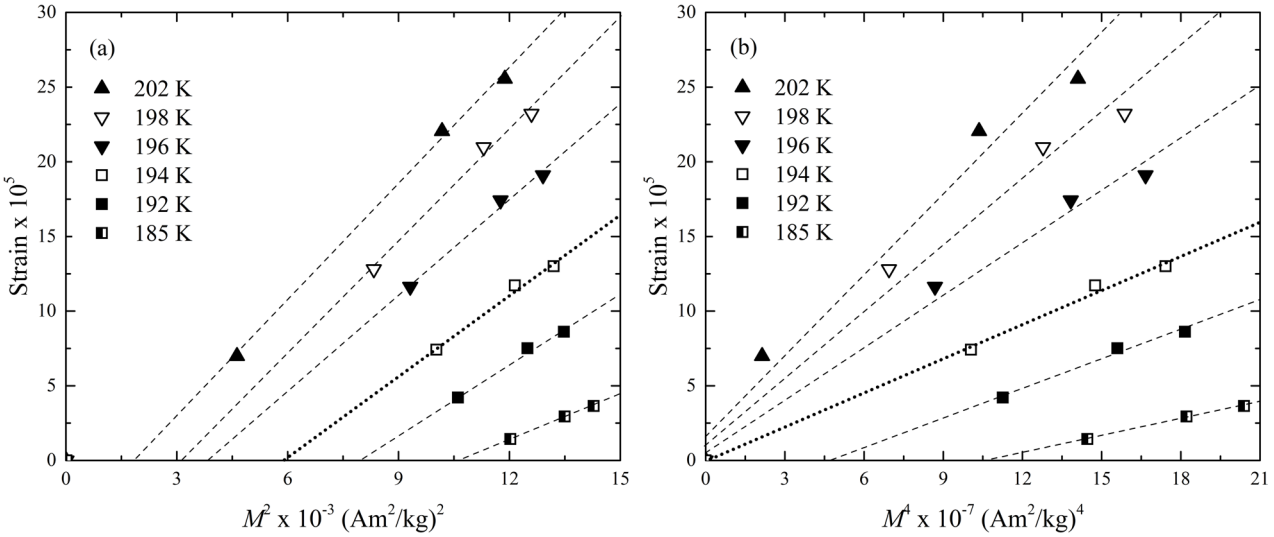

Figure 8. Forced magnetostriction $\Delta L/L$ of $LaFe_{11.6}Si_{1.4}$ determined from magnetic field-dependent XRD (a) as a function of M^2 and (b) as function of M^4. The dashed straight lines are linear fits for each temperature and the dotted line highlights the linear fit at $T_C = 194$ K.

[28, 30]. Since ξ increases, we expect an increasing magnetic pressure on cooling and a larger effect on a(PM) closer to T_C. From our data we find that both ξ and a(PM) increase upon cooling and sharply close to T_C, verifying the theory of internal magnetic pressure. The deviation from linear thermal contraction of $LaFe_{11.6}Si_{1.4}$ can therefore be seen as another measure of ξ.

4.3. Correlation between magnetization and critical forced magnetostriction

In order to probe the magnetization dependence of critical forced magnetostriction according to equation (1), we extracted lattice parameters of $LaFe_{11.6}Si_{1.4}$ powder from Rietveld refinements of our magnetic field and temperature-dependent x-ray diffraction measurements. We derived the forced magnetostriction $\Delta L/L$ from the relative change in lattice parameter in magnetic field compared to zero-field data. The resulting $\Delta L/L$ is shown as a function of M^2 and M^4 in figures 8(a) and (b), respectively. Magnetization measurements performed separately for $LaFe_{11.6}Si_{1.4}$ powder confirm a broadening of the transition and a slightly larger $T_C = 194$ K, which is still very close to the bulk value.

Classical SEW theory of magnetovolume coupling (neglecting fluctuations) suggests that $\Delta L/L$ versus M^2 follows a straight line through the origin at T_C [47]. The forced magnetostriction of $LaFe_{11.6}Si_{1.4}$ indeed follows a straight line versus M^2 for all temperatures close to T_C, see figure 8(a), however, for none through the origin. This observation is in accordance with Takahashi's SCR spin fluctuation theory. He suggests a change from M^2-linearity behavior to M^4-linearity behavior at T_C, as shown in equation (1) [20]. The plot of $\Delta L/L$ versus M^4, see figure 8(b), indeed indicates linearity through the origin at T_C.

5. Conclusions

Neutron and x-ray diffraction studies on $LaFe_{11.6}Si_{1.4}$ reveal that short-range magnetic correlations in the paramagnetic regime drive the first-order PM–FM transition. These spin fluctuations are observable as neutron diffuse scattering and exist as far as 100 K above the Curie temperature $T_C = 190$ K. On cooling, the magnetic diffuse intensity I_{diff} and *ac* magnetic susceptibility χ show the same temperature dependence. I_{diff} is, therefore, directly related to the amplitude of short-range magnetic correlations ξ. ξ increases as T_C is approached, creating an internal magnetic pressure that leads to a deviation from linear thermal contraction and an overcompensation close to T_C. Both the PM and FM phase coexist in the temperature range between $T_{tr} = 200$ K and T_C, in which I_{diff} in the neutron diffraction patterns is transferred to magnetic Bragg intensity I_{mag}. The lattice parameter of PM phase increases sharply in the two-phase region, simultaneously to a large increase in ξ—verifying the pressure effect created by the spin fluctuations. The critical forced magnetostriction at T_C is proportional to the fourth power of magnetization, which is in accordance with Takahashi's SCR spin fluctuation theory.

Paramagnetic spin fluctuations might in general play an important role in driving the magnetocaloric effect in $LaFe_{13-x}Si_x$. We expect that the fluctuations are increasingly suppressed with larger Si concentrations x, especially for compositions $x > 1.6$, which have a second-order transition. However, the evolution of spin fluctuations in the $LaFe_{13-x}Si_x$

system as function of x and, consequentially, the extension to the commercially applied $La(Fe,Mn)_{13-x}Si_xH_y$ system would be a topic for further investigation. It could provide a generalized view on the occurrence of the GME.

Acknowledgments

We would like to thank LVB Diop for performing the magnetic calculations and helpful discussions regarding the manuscript and DFG instrument grant INST 163/442-1 FUGG and LOEWE RESPONSE for funding.

ORCID iDs

Tom Faske https://orcid.org/0000-0002-7073-0864

References

[1] Fujita A, Fujieda S, Fukamichi K, Mitamura H and Goto T 2001 *Phys. Rev.* B **65** 131
[2] Fujieda S, Fujita A and Fukamichi K 2002 *Appl. Phys. Lett.* **81** 1276–8
[3] Pecharsky V K and Gschneidner K A Jr 1999 *J. Magn. Magn. Mater.* **200** 44–56
[4] Gschneidner K A and Pecharsky V K 1999 *J. Appl. Phys.* **85** 5365–8
[5] Pecharsky V K and Gschneidner K A 2001 *J. Appl. Phys.* **90** 4614–22
[6] Liu J, Gottschall T, Skokov K P, Moore J D and Gutfleisch O 2012 *Nat. Mater.* **11** 620–6
[7] Yamada H 1993 *Phys. Rev.* B **47** 11211–9
[8] Fujita A, Akamatsu Y and Fukamichi K 1999 *J. Appl. Phys.* **85** 4756–8
[9] Jia L, Liu G J, Sun J R, Zhang H W, Hu F X, Dong C, Rao G H and Shen B G 2006 *J. Appl. Phys.* **100** 123904
[10] Fujita A and Yako H 2012 *Scr. Mater.* **67** 578–83
[11] Fujita A and Fukamichi K 1999 *IEEE Trans. Magn.* **35** 3796–8
[12] Wang F, Wang G-J, Hu F-X, Kurbakov A, Shen B-G and Cheng Z-H 2003 *J. Phys.: Condens. Matter* **15** 5269–78
[13] Rosca M, Balli M, Fruchart D, Gignoux D, Hlil E K, Miraglia S, Ouladdiaf B and Wolfers P 2010 *J. Alloys Compd.* **490** 50–5
[14] Fujita A 2016 *APL Mater.* **4** 64108
[15] Palstra T T M, Mydosh J A, Nieuwenhuys G J, van der Kraan A M and Buschow K H J 1983 *J. Magn. Magn. Mater.* **36** 290–6
[16] Fujita A, Fukamichi K, Yamada M and Goto T 2006 *Phys. Rev.* B **73** 167
[17] Fujita A, Yako H and Kano M 2013 *J. Appl. Phys.* **113** 17A924
[18] Bean C P and Rodbell D S 1962 *Phys. Rev.* **126** 104–15
[19] Takahashi Y and Moriya T 1985 *J. Phys. Soc. Japan* **54** 1592–8
[20] Takahashi Y 2013 *Spin Fluctuation Theory of Itinerant Electron Magnetism* (*Springer Tracts in Modern Physics, 0081-3869* vol 253) (Heidelberg: Springer) (https://doi.org/10.1007/978-3-642-36666-6)
[21] Amaral V S and Amaral J S 2004 *J. Magn. Magn. Mater.* **272–6** 2104–5
[22] Zarifi M, Kameli P, Mansouri M, Ahmadvand H and Salamati H 2017 *Solid State Commun.* **262** 20–8
[23] Miao X F *et al* 2016 *Phys. Rev.* B **94** 14426
[24] Miao X F, Caron L, Gubbens P C M, Yaouanc A, Dalmas de Réotier P, Luetkens H, Amato A, van Dijk N H and Brück E 2016 *J. Sci., Adv. Mater. Devices* **1** 147–51
[25] Kanomata T, Sasaki T, Nishihara H, Yoshida H, Kaneko T, Hane S, Goto T, Takeishi N and Ishida S 2005 *J. Alloys Compd.* **393** 26–33
[26] Sakon T, Hayashi Y, Fujimoto N, Kanomata T, Nojiri H and Adachi Y 2018 *J. Appl. Phys.* **123** 213902
[27] Shigeta I *et al* 2018 *Phys. Rev.* B **97** 104414
[28] Wagner D and Wohlfarth E P 1986 *Phys. Lett.* A **118** 29–31
[29] Moriya T and Kawabata A 1973 *J. Phys. Soc. Japan* **34** 639–51
[30] Mohn P, Wagner D and Wohlfarth E P 1987 *J. Phys. F: Met. Phys.* **17** L13–8
[31] Wada H, Nakamura H, Fukami E, Yoshimura K, Shiga M and Nakamura Y 1987 *J. Magn. Magn. Mater.* **70** 17–9
[32] Takahashi Y 1986 *J. Phys. Soc. Japan* **55** 3553–73
[33] Squires G L 2012 *Introduction to the Theory of Thermal Neutron Scattering* 3rd edn (Cambridge: Cambridge University Press) (https://doi.org/10.1017/cbo9781139107808)
[34] Krautz M, Skokov K, Gottschall T, Teixeira C S, Waske A, Liu J, Schultz L and Gutfleisch O 2014 *J. Alloys Compd.* **598** 27–32
[35] Hoelzel M, Senyshyn A, Juenke N, Boysen H, Schmahl W and Fuess H 2012 *Nucl. Instrum. Methods Phys. Res.* A **667** 32–7
[36] Rietveld H M 1969 *J. Appl. Crystallogr.* **2** 65–71
[37] Rodríguez-Carvajal J 1993 *Physica* B **192** 55–69
[38] Faske T and Donner W 2018 *J. Appl. Crystallogr.* **51** 761–7
[39] Momma K and Izumi F 2011 *J. Appl. Crystallogr.* **44** 1272–6
[40] Fujieda S, Fujita A, Fukamichi K, Yamaguchi Y and Ohoyama K 2008 *J. Phys. Soc. Japan* **77** 74722
[41] Moriya T 1979 *J. Magn. Magn. Mater.* **14** 1–46
[42] Moriya T 1991 *J. Magn. Magn. Mater.* **100** 261–71
[43] Kübler J 2000 *Theory of Itinerant Electron Magnetism* (Oxford: Oxford University Press)
[44] Gottschall T, Benke D, Fries M, Taubel A, Radulov I A, Skokov K P and Gutfleisch O 2017 *Adv. Funct. Mater.* **27** 1606735
[45] Chatterji T 2006 *Neutron Scattering from Magnetic Materials* (Amsterdam: Elsevier) (https://doi.org/10.1016/b978-0-444-51050-1.x5000-9)
[46] Kubo R 1966 *Rep. Prog. Phys.* **29** 255–84
[47] Edwards D M and Wohlfarth E P 1968 *Proc. R. Soc.* A **303** 127–37